DOI: 10.18721/JCSTCS.14204
УДК 621.3

MEMS ALKALI VAPOR CELL ENCAPSULATION TECHNOLOGIES FOR CHIP-SCALE ATOMIC CLOCK

A.N. Kazakin[1], R.V. Kleimanov[1], A.V. Korshunov[1], Yu.D. Akulshin[1], A.V. Shashkin[2]

[1] Peter the Great St. Petersburg Polytechnic University, St. Petersburg, Russian Federation;

[2] S.I. Vavilov State Optical Institute, St. Petersburg, Russian Federation

The article is dedicated to solving the problem of creation of small-size quantum frequency standards for telecommunications and navigation systems using the methods of MEMS technologies. The analysis of the conventional MEMS atomic clocks operating on the effect of coherent population trapping shows that the conditions of the technological operation for alkali vapor cells sealing have the greatest influence on the clock performance. To improve the atomic clock short-term and long-term frequency stability, it is necessary to reduce the cell sealing temperature and use materials with low gas permeability. Therefore, experimental work was carried out to find new structural materials for the atomic cell design and two MEMS technologies of low-temperature anodic bonding were developed. The first one is based on the use of transparent glass-ceramics SO-33M and provides anodic sealing at a temperature of 150 °C. Using this technology, prototypes of MEMS cells with optical windows made of glass-ceramic and fused quartz were made. The second technology is based on the anodic bonding of LK5 glass and silicon at a temperature of 250 °C and was used to fabricate MEMS cells filled with vapors of rubidium-87 or caesium-133 isotopes in neon buffer gas.

Keywords: MEMS atomic clock, alkali vapor cell, anodic bonding, glass, glass-ceramics, quantum frequency standard.

Citation: Kazakin A.N., Kleimanov R.V., Korshunov A.V., Akulshin Yu.D., Shashkin A.V. MEMS alkali vapor cell encapsulation technologies for chip-scale atomic clock. Computing, Telecommunications and Control, 2021, Vol. 14, No. 2, Pp. 49–64. DOI: 10.18721/JCST-CS.14204

ТЕХНОЛОГИИ ГЕРМЕТИЗАЦИИ ЩЕЛОЧНОЙ ГАЗОВОЙ МЭМС-ЯЧЕЙКИ ДЛЯ МИНИАТЮРНЫХ АТОМНЫХ ЧАСОВ

А.Н. Казакин[1], Р.В. Клейманов[1], А.В. Коршунов[1], Ю.Д. Акульшин[1], А.В. Шашкин[2]

[1] Санкт-Петербургский политехнический университет Петра Великого, Санкт-Петербург, Российская Федерация;

[2] Государственный оптический институт им. С.И. Вавилова, Санкт-Петербург, Российская Федерация

Статья посвящена решению проблемы создания малогабаритных квантовых стандартов частоты для телекоммуникационных и навигационных систем при помощи методов МЭМС-технологий. Анализ существующих конструкций МЭМС атомных часов, рабо-

тающих на эффекте когерентного пленения населенностей, показал, что наибольшее влияние на их метрологические характеристики оказывают условия проведения операции герметизации парощелочных атомных ячеек. Для повышения точности и долговременной стабильности МЭМС часов необходимо уменьшать температуру этой операции и применять материалы с низкой газопроницаемостью. Поэтому была проведена экспериментальная работа по поиску новых конструкционных материалов для атомной ячейки и разработаны две технологии низкотемпературной анодной термодиффузионной герметизации. Первая основана на применении прозрачной стеклокерамики СО-33М и позволяет проводить анодную герметизацию при температуре 150 °С. По этой технологии изготовлены прототипы МЭМС-ячеек с окнами из стеклокерамики и плавленого кварца. Вторая технология, основанная на анодном соединении стекла ЛК5 и кремния при 250 °С, использована для изготовления действующих образцов МЭМС-ячеек, заполненных парами изотопов рубидия-87 или цезия-133 и буферным газом неоном.

Ключевые слова: МЭМС, атомные часы, щелочная ячейка, анодная сварка, стекло, стеклокерамика, квантовый стандарт частоты.

Ссылка при цитировании: Kazakin A.N., Kleimanov R.V., Korshunov A.V., Akulshin Yu.D., Shashkin A.V. MEMS alkali vapor cell encapsulation technologies for chip-scale atomic clock // Computing, Telecommunications and Control. 2021. Vol. 14. No. 2. Pp. 49–64. DOI: 10.18721/JCSTCS.14204

Introduction

The application fields of quantum devices with optical pumping is expanding every year: from telecommunication, network synchronization and satellite navigation systems [1–3] to medical diagnostics [4], atomic spectroscopy [5] and quantum-enhanced metrology systems based on ensemble of ultra cold atoms [6]. The success achieved in the miniaturization of quantum devices and the development of standardized methods of physics packaging of optical component with electronics ensured their mass production [7–10]. Development of technologies of microelectromechanical systems (MEMS) and vertical-cavity surface-emitting lasers (VCSEL) made it possible to create miniature atomic magnetometers and chip-scale atomic clocks (CSAC) based on the coherent population trapping (CPT) effect [11–13].

A key element of modern quantum devices is millimeter-size atomic cells containing alkali metal vapors in inert atmosphere or vacuum [1, 14, 15]. To increase the atomic quality factor and reduce frequency instability of CSAC, different buffer gases or organic anti-relaxation coatings of the inner walls of the cell are used [16, 17]. Benefiting from planar MEMS technologies, MEMS cells are characterized by small size, flat optical windows, low fabricating cost, and provide low power consumption and simplicity of integration with other components of CSAC (thin film heaters, anti-reflective coatings, optical filters, microlens, etc.) [12].

The MEMS cells are formed by sandwiching a silicon wafer with through-hole cavity between two transparent glass wafers. The main processes of the MEMS cells technology are optical cavities formation, filling with an alkali metal source and vacuum-tight sealing of the cell in the appropriate buffer atmosphere [18]. Optical cavities are implemented by dry or wet through-wafer etching of silicon. Pure alkali metals or alkali salts with reducing agent are used as vapors sources.

Vacuum-tight sealing is the main MEMS technology that has the greatest impact on the atomic cell performance. For hermetic sealing of such devices on a wafer level, various bonding technologies are used, the most widespread of which is the anodic bonding of silicon and glass wafers [19]. Anodic bonding is based on electro-chemical processes taking place between joined surfaces at elevated temperatures and under action of electric field [20]. Materials for the anodic bonding are special borosilicate glasses (Borofloat 33, Pyrex 7740), which have high ionic conductivity at bonding temperatures, optical transparency and coefficient of thermal expansion (CTE) approximately matched to CTE of silicon. At the

same time, high temperatures (300–500 °C) required for high-quality anodic bonding silicon to borosilicate glasses, limit the application of this technology for sealing of some types of MEMS atomic cells due to low dissociation temperatures of alkali salts or organic anti-relaxation coatings and the difficulty of providing the exact composition and pressure of buffer atmosphere.

This paper presents the results of the development of the low temperature anodic bonding technology for vacuum-tight sealing of MEMS atomic cells, developed jointly by Higher School of Applied Physics and Space Technologies and Laboratory of Nano- and Microsystem Technology of Peter the Great St. Petersburg Polytechnic University.

The dependence of the atomic clock performance on the MEMS cell design

The short-term frequency stability and long-term frequency stability are two main factors that determine the atomic clock performance. Both these values are interrelated and directly depend on the dimensions and materials of vapor cell, the alkali metal used and the inner atmosphere composition.

In MEMS cells, ^{87}Rb and ^{133}C isotopes are usually used to observe the CPT-resonance at D1 reference transition (when optical pumping at D2 line is used, the resonance contrast does not exceed several percent due to the strong broadening of the optical transitions in collisions of atoms with buffer gas molecules and the difference in the probabilities of the corresponding electrodipole transitions). Instead of pure alkali metals due to their low melting point, alkali azide salts or solid microdispensers based on alkali chlorides and chromates with reducing agent are used as vapors sources in the MEMS cell designs. The release of alkali metal vapors is carried out after the vacuum-tight cell encapsulation as a result of a chemical reaction by local heating or salt dissociation under the influence of UV light [1, 18]. For this reason, modern MEMS cells in most cases have a two-chamber design, which consist of optical and dispenser cavities with a volume of several cubic millimeters connected by narrow filtration channels.

Fig. 1 shows two possible designs of two-chamber cell that can be fabricated using low-cost MEMS technologies. The first design is made by the classic glass-silicon-glass technology, which uses anodic bonding to connect all parts (Fig. 1*a*). In this variant, the optical path size is about 1 mm, since it is limited by the existing technological capabilities to etch through-wafer cavities in a thick silicon substrate. The second one is an all-glass cell (Fig. 1*b*). In this variant, anodic sealing of the cell is carried out through thin intermediate layers (such as Si, SiC, Al films with sub-micrometer thickness) deposited on the surface of the glasses [21, 22]. The dimensions of such cells can be more than 5 mm, which is due to high rates of mechanical or abrasive micromachining of glasses [8, 9].

When the size of the gas cells is reduced to millimeter scale, the absorption of the optical pumping is significantly reduced. This fact leads to the need to warm up the cells to temperatures of 80–120 °C, which reduces short-term frequency stability. At present, the relative short-term frequency stability of the CSAC is significantly less than this value for conventional atomic clocks based on glass-blown cells. Because of a major contribution to the CPT linewidth are collisions of the alkali atoms with the cell walls, which completely depolarize the spin of the atoms, frequency stability of the clock degrades with smaller size. To reduce this effect, a buffer gas is added to the vapor cell to narrow the transition linewidths [16, 23]. Gases such as He, Ne, Ar, and N_2 interact only very weakly with the spin of the alkali atoms and hence the atoms can undergo thousands collisions with the buffer gas before the spin depolarizes. At the same time it shifts the hyperfine frequency and this shift is temperature-dependent, which impairs the CSAC long-term frequency stability due to temperature fluctuations [24]. The value and sign of the temperature shift of the reference transition depend on the composition and pressure of the buffer gas, which makes it necessary to carefully select the components of the inert atmosphere to minimize this negative phenomenon [14]. At present, the relative short-term frequency stability of the CSAC with buffer-gas atomic cells is 10^{-10}–10^{-11} $s^{-1/2}$, and drift rates are 10^{-8}–10^{-11}/day [1].

An alternative approach to reduce the effects of wall collisions is to apply an anti-relaxation coating such as straight-chain alkanes, alkenes, and organochlorosilanes on the inner walls of the vapor cell [17,

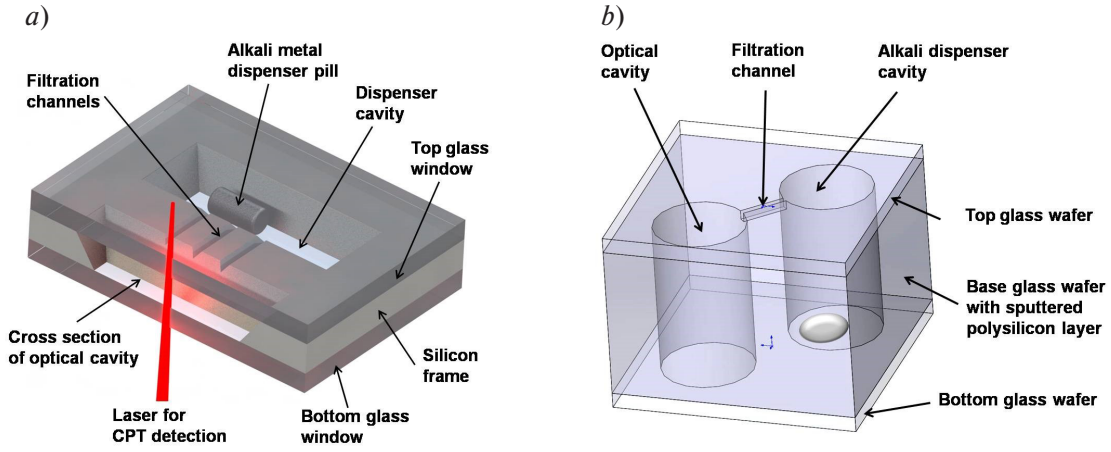

Fig. 1. Two-chamber cell schemes: glass-silicon-glass cell (*a*) and all-glass cell (*b*)

25–27]. In this variant, the rate of relaxation of the spin-polarized alkali atoms when they collide with the wall of the absorption chamber is reduced by four orders of magnitude. Experiments show that the anti-relaxation coating also leads to shifts in the frequency of the reference transition, but these shifts drift very slowly over time (less than 10 Hz over a time span of 30 years). This feature of coated cells is very useful for atomic frequency standards in deep space communications and GLONASS systems. It is pertinent to note that buffer-gas-free cells with anti-relaxation coatings so far have not been used in commercial atomic clocks due to decomposition of the organic coating at high temperatures required by anodic bonding process used in micro-fabrication of MEMS vapor cells [25]. However, recent studies have shown that the coating based on octadecyltrichlorosilane (OTS) can be compatible with MEMS cell technology if it is possible to lower the anodic sealing temperature to 170 °C [26, 27].

The materials of the cell walls and thin optical windows affect the long-term frequency stability of CSAC. The gas permeability of borosilicate glasses for helium and neon leads to a change in the composition of the buffer atmosphere inside the MEMS cell over time [6, 28–30]. As experiments show, for a millimeter-size cell with Cs-Ne vapor, the frequency shift due to the gas permeability of the Borofloat 33 glass is about $-5 \cdot 10^{-11}$/day [29]. Replacing conventional borosilicate glasses with more expensive aluminosilicate glasses can reduce long-term frequency instability by several orders of magnitude [30].

Selection of materials for anodic sealing of MEMS cell

In the frame of this work, we tested alternative anodic bonding materials, which are promising for the fabrication technology cost reducing and the cell performance improving. One of them is LK5 glass, which is a domestic analog of Borofloat® 33 glass (Schott). Both glasses have approximately the same coefficients of thermal expansion, close to single-crystal silicon, but their compositions are slightly different [31].

The second tested material is SO-33M glass-ceramic (commercial name is “CO-33M”, provided by S.I. Vavilov State Optical Institute data, St. Petersburg, Russia). This is a transparent glass-ceramic (TGC) synthesized on the basis of lithium aluminosilicates which has an average CTE close to zero and is close in its characteristics to the Zerodur® glass-ceramic (Schott). The coefficient of thermal expansion of the SO-33M glass-ceramic used in this work is far from silicon CTE, but it is matched with fused quartz in a wide temperature range. Therefore, this material can only be used for the fabrication of all-glass-ceramic cells or cells with quartz windows. The Table 1 shows a comparison of the mechanical, optical and technological parameters of SO-33M glass-ceramic and Borofloat 33 glass, which are important for the technology of MEMS atomic cells. Lithium aluminosilicates transparent glass-ceramics can become good alternative materials for anodic sealing of MEMS because they have many advantages

over glasses – high working temperature, low gas permeability, low fragility, high strength, thermal shock resistance, durability during mechanical processing [32]. Lithium ions in the glass and glass-ceramics have an increased ionic mobility compared to sodium ions [33]. For this reason, such materials can be bonded at lower temperatures than conventional borosilicate glasses [34].

The optical transmittance of SO 33M, LK5 and Borofloat 33 wafers with a thickness of 450–500 μm has been measured by spectrophotometer Shimadzu uv 3600. The spectral dependences prove an almost complete identity of the transmittance of both LK5 and Borofloat 33 glasses in the wavelengths range of 300–3000 nm. The SO 33M glass-ceramic transmits light only 2 % worse than Borofloat 33 in the range of 500–2500 nm.

Table 1

Comparison of glass and glass-ceramic parameters for MEMS sealing

	Borofloat 33 glass*	SO-33M glass-ceramic**
CTE, 10^{-6} 1/K (20–300 °C)	3.25	~ 0.5 –0.15–0.1 (in 60–100 °C)
Maximal working temperature, °C	500	700
Density ρ, g/cm^3	2.2	2.5
Hardness	480 (HK0.1/20)	> 750 (HB)
Young's Modulus E, GPa	64	83
Poisson's ratio μ	0.2	0.27
Helium permeability, Pa·m^3/s (200 °C)	~ 10–9	< 10–11
Refractive index n_d	1.47	1.54
Transmittance in 500–2500 nm, % *** (for wafer with thickness of 0.5 mm)	92.5	90.5
at 795 nm (^{87}Rb D1 line) ***	92.34	90.69
at 780 nm (^{87}Rb D2 line) ***	92.39	90.70
at 895 nm (^{133}Cs D1 line) ***	92.48	90.55
at 852 nm (^{133}Cs D2 line) ***	92.35	90.67
MEMS technology compatibility ***: Anodic bonding temperatures, °C Chemical etching in HF solutions Electro-discharge drilling in NaOH Laser micromachining Microdrilling	 300–450 excellent excellent poor poor	 150–300 poor poor good excellent

* – Schott data; ** – S.I. Vavilov State Optical Institute data; *** – Authors data

Anodic bonding experiments

The principle of the anodic bonding process is shown in Fig. 2*a*. The silicon wafer is connected to a flat metal anode and the top glass wafer is connected to a needle or thin-film cathode. The stacked wafers are heated up by a hot plate. When the bonding temperature is reached, the bonding voltage is applied to the contacted wafer. The electric field causes the dissociated alkali cations in the glass to move

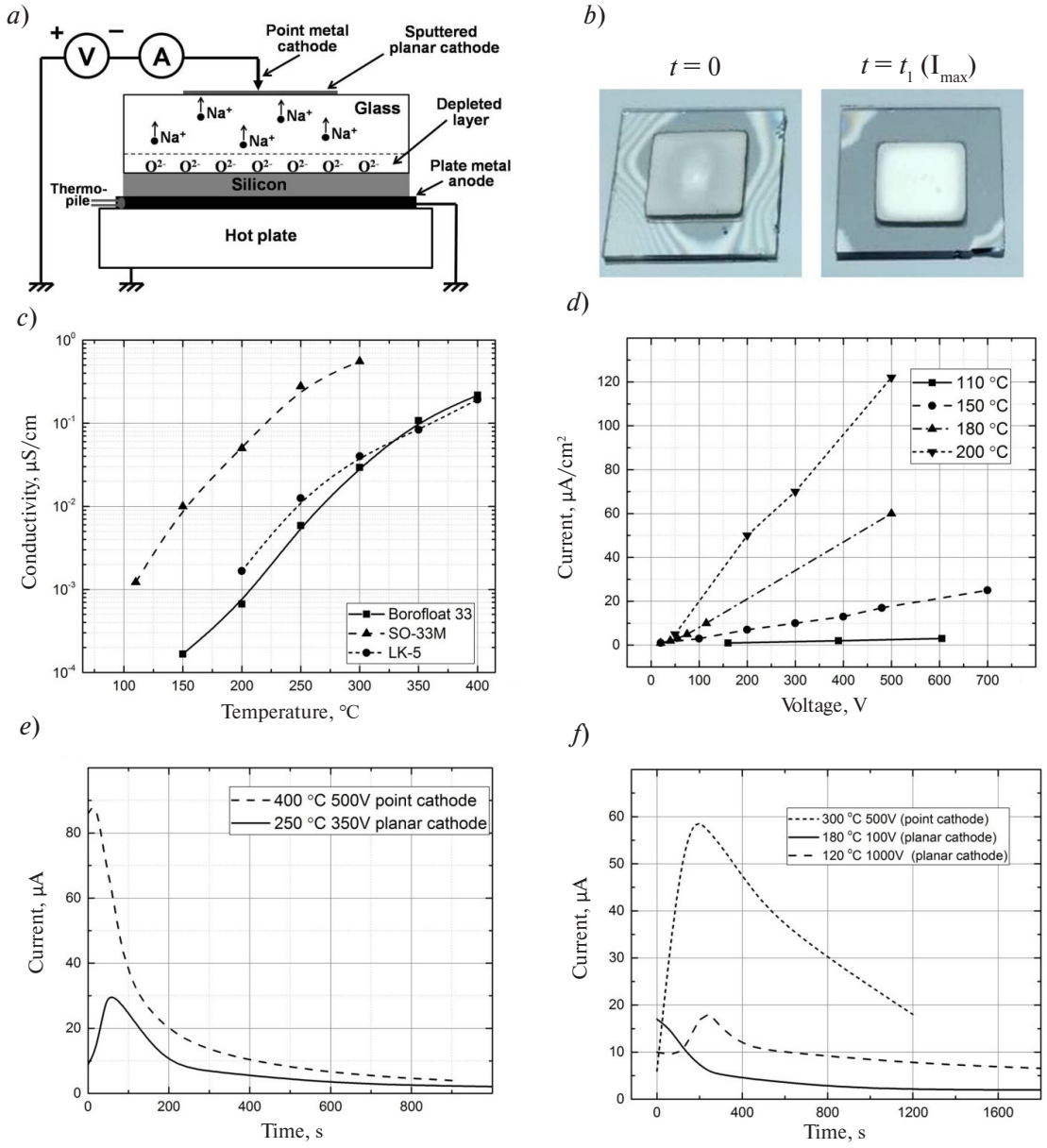

Fig. 2. Anodic bonding experiments results: bonding scheme (*a*), samples view at different bonding stages (*b*), samples conductivities (*c*), SO-33M current-voltage dependencies (*d*), current responses during bonding of silicon to LK5 (*e*) and SO 33M (*f*)

towards the cathode, forming a depleted region at the glass-silicon interface. When the bond pair makes intimate contact, the chemical reaction takes place at the interface, resulting in the oxidation of the silicon substrate and consequently realizing a permanent bond between the glass and the silicon. As shown in Fig. 2*b*, during the bonding process, Newton's rings were observed at the beginning between the glass and silicon surfaces. After the voltage is applied, an enlargement of the reaction area was observed.

Both LK5 glass and SO-33M glass-ceramic materials are firstly characterized through the experimental way.

The measurement of the glass and glass-ceramic electrical conductivity was carried out in laboratory equipment designed for silicon-glass anodic bonding. The 500 μm thick wafers were preliminarily divided into square samples with an area of 1 cm^2, cleaned in piranha solution and rinsed in deionized

water, and thin-film aluminum electrodes were deposited on both sample sides by DC-magnetron sputtering. The initial current peak value at the moment of switching on the voltage was used to estimate the samples conductivity at a given temperature. The obtained temperature dependencies of the samples conductivity in comparison with the Borofloat 33 glass are shown in Fig. 2*c*.

At standard bonding temperatures (> 350 °C), the conductivities of both LK5 and Borofloat 33 glasses are approximately equal. However, in the temperature range of 200–300 °C, the ionic conductivity of LK5 glass exceeds the Borofloat 33 one by about two times. This fact is important for the cell sealing in neon atmosphere at pressures of several hundred Torr, because it allows us to achieve a hermetic silicon-LK5 bonding at lower temperatures and volts.

The SO-33M glass-ceramic conductivity were 2 to 3 orders of magnitude higher than that of Borofloat 33 glass in the entire temperature range studied. This case made it possible to carry out an anodic bonding of TGC samples to each other at a temperature of about 150 °C.

Time dependencies of the current density during anodic bonding of LK5 and SO-33M to silicon at different bonding conditions are shown in Fig. 2*e* and Fig. 2*f*, respectively. The time evolution of bonding current and the area under these curves, which equal to the total charge passed through the glass-silicon interface, are the criteria for the bonding quality evaluation. Minimal charge density sufficient to create a bond between the Si and the glass is 3 mC/cm^2 [22]. At low temperatures (less than 270 °C and 180 °C for LK5 and SO 33M, respectively) and using a point cathode, the passed charge density is insufficient for the depleted layer formation and high-quality bonding. To increase this value and provide a durable bonding at low temperatures, it is necessary to use a thin-film cathode with a large area or increase the bonding voltage (Fig. 2*d*).

The duration of the process, sufficient to provide a uniform bonding over the entire wafers area, was estimated by the time response of the current. The increase in the current in the first minutes of bonding was due to the spreading of the joint spot over most of the silicon sample area under the influence of electrostatic force, as shown in right side of Fig. 2*b*. After that, all current responses for LK5 bonding showed a purely ionic character of conductivity with exponential current drop over time, which indicates the fast formation of a depleted layer (Fig. 2*e*). In most cases, twenty minutes was enough for LK5-to-silicon bonding of the wafers with a diameter of 3″. The behavior of current during glass-ceramic bonding was more complex and its drop over time was slower (Fig. 2*f*). This circumstance required an increase in the TGC-to-silicon bonding duration up to one hour.

The results of this characterization work provided an overview of bonding parameters for both materials and were used in the development of MEMS cell fabrication process.

Anodic sealing of glass-silicon-glass sandwich and sandwich of three glass-ceramic wafers using intermediate polysilicon layers has been carried out in a lab tool that provides a gap between the wafers for vacuuming and degassing the cells cavities. The tool with attached wafers was placed in a vacuum cham-

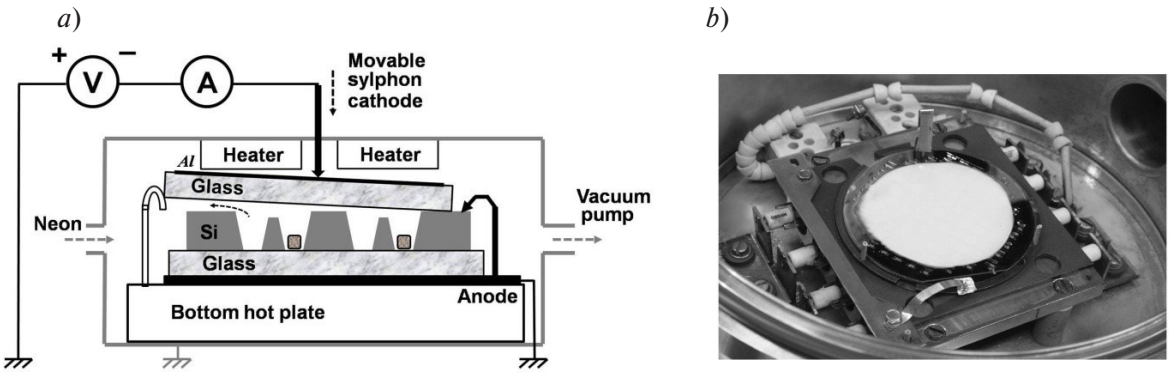

Fig. 3. Gas cells sealing equipment scheme (*a*) and bonding tool view (*b*)

ber equipped with a gas line for the supply of inert gases. The scheme of bonding equipment and real view of tool with bonded wafers in the vacuum chamber are shown in Fig. 3*a* and Fig. 3*b*, respectively.

In the case of bonding of glass-ceramic wafers to each other, one of the wafers acted as a silicon wafer in scheme shown in Fig. 3*a*, but its conductivity was provided by thin-film conductive layers deposited on bottom and top wafer surfaces. To perform this process polysilicon films with a thickness of 200 nm and resistivity of approximately 600 Ohm·cm was deposited by DC-magnetron sputtering from a single-crystal silicon target with a resistivity of 0.1 Ohm·cm. The glass or TGC top wafer shifted slightly to the side in order to spare place for the point anode contact to the polysilicon layer or silicon wafer.

Development of anodic sealing technology for glass-ceramic atomic cells

This configuration of bonding equipment was used to fabricate a prototype of two-chamber all–glass-ceramic cell, shown in Fig. 1*b*. The cell was formed by sandwiching a glass-ceramic wafer with two through-hole cavities and connection channels between two another wafers by anodic bonding using polysilicon interlayers. Thickness of TGC wafers was 500 μm. Cell fabrication process is shown in Fig. 4.

First glass-ceramic wafer micromachining was carried out by drilling with tubular drills with diamond grains binded by electroplating (Fig. 4*a*). The drills diameter was 2 and 3 mm. The wafer was fixed to the movable substrate holder by molten paraffin. The cavities formation was carried out by through-wafer sinking the drill bit at spin rate of 1000 rpm. Formation of two arc-shaped channels with a width of 200 μm was carried out by sinking the tubular drill to the depth of 150 μm at the center point between the cavities. After removing the paraffin in toluene, the wafer was cleaned in isopropanol, water and piranha solution. Then 200 nm thick polysilicon films were sputtered on both sides of the wafer (Fig. 4*b*).

First anodic bonding was carried out to join the micromachined wafer to the bottom TGC wafer (Fig. 4*c*). This operation was performed in air condition at 250 °C and 500 V using a point cathode to visually observe the formation of a bonding spot. The operation of the filling the cell with an alkali dispenser was not performed at the prototype fabrication stage. Second anodic bonding at the same conditions was carried out to seal the cell by top TGC wafer (Fig. 4*d*). Drop of the current passed through the interface during the first and second anodic bonding are shown in Fig. 5*b*.

The behavior of the second bonding current did not show a fast exponential drop. This may be due to the high surface resistance of polysilicon layer, comparable to the resistance of a bulk SO-33M wafer at bonding temperature used. As a result, part of the anode current is provided by the ion flow in the bottom glass-ceramic wafer. Despite this, the anodic sealing was successful. Prototype of a sealed glass-ceramic cell with dimensions of 10 × 10 × 1.5 mm is shown in Fig. 5*a*.

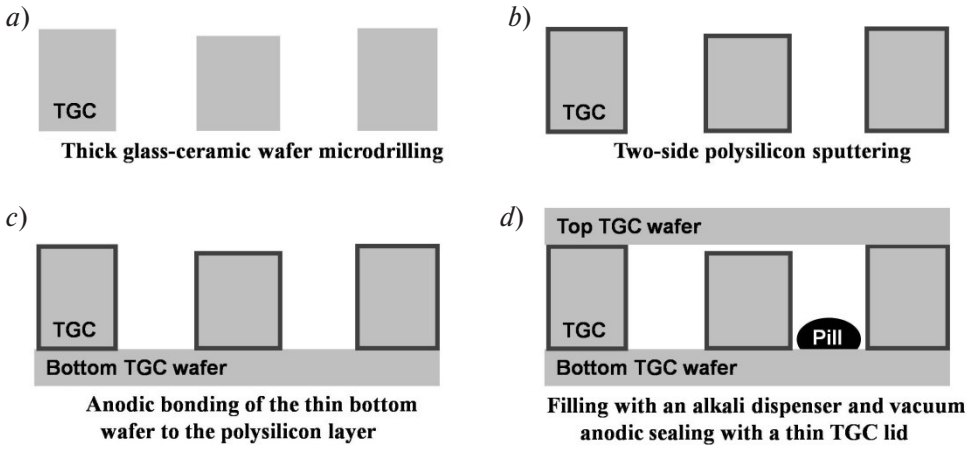

Fig. 4. Glass-ceramic MEMS cell fabrication process

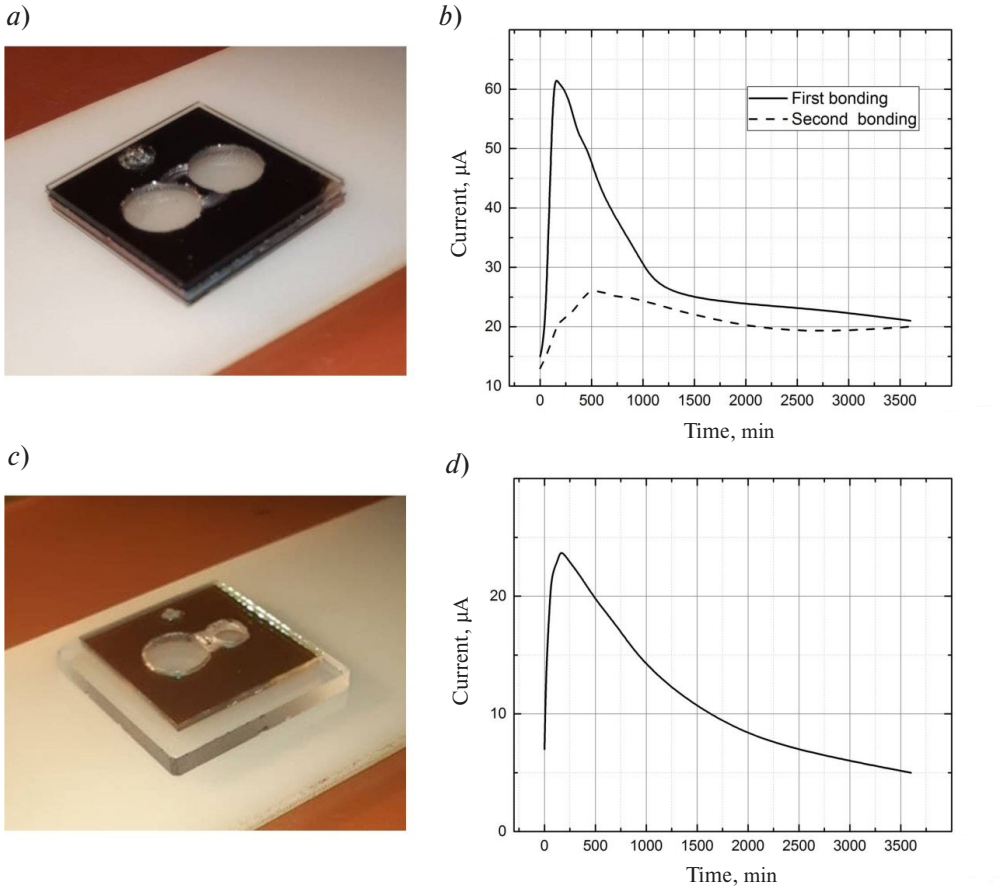

Fig. 5. Sandwich of three SO-33M glass-ceramic samples bonded through polysilicon films (*a*) and bonding currents responses (*b*); bonded sandwich of SO-33M and 1 mm thick fused quartz (*c*) and bonding current response (*d*)

The same bonding conditions were applied to bond SO-33M glass-ceramic to fused quartz due to the proximity of their CTE. A polysilicon layer was deposited on the quartz sample. The bonding process was accompanied by normal current behavior over time (Fig. 5*d*). The bonded TGC-quartz sandwich after etching of the polysilicon layer in the optical cavities is shown in Fig. 5*c*.

In addition to alkali vapor cell technology such technology may be also promising for manufacturing of atomic cells with Hg vapors. However, for low-temperature sealing of MEMS atomic cells with anti-relaxation coatings, described fabrication process requires further optimization.

Fabrication of MEMS alkali vapor cells with neon buffer gas

Vacuum-tight silicon-to-LK5-glass anodic bonding in neon atmosphere has been successfully applied to fabricate the Cs-Ne and Rb-Ne atomic cells (Fig. 6).

The cells fabrication process and the view of 3″ wafer containing a hundred cells are shown in Fig. 6*a* and Fig. 6*b*, respectively.

The cells were made in the form of chips with a total size of 6 × 6 × 1.6 mm. The basic cell design contained two volumetric cavities with sizes of 3 × 1.5 × 0.6 mm, connected by rectangular channels with a length of 1 mm and a width of 100 or 200 μm (Fig. 6*c*). Depending on the manufacturing conditions, the real appearance of the chips could differ from the basic design (Fig. 6*d–f*).

A (100)-oriented 3″ silicon wafer with a thickness of 400–600 μm and two LK5 glass wafers with a thickness of 450–500 μm are used for cells fabricate. The both surfaces of the wafers were polished prior

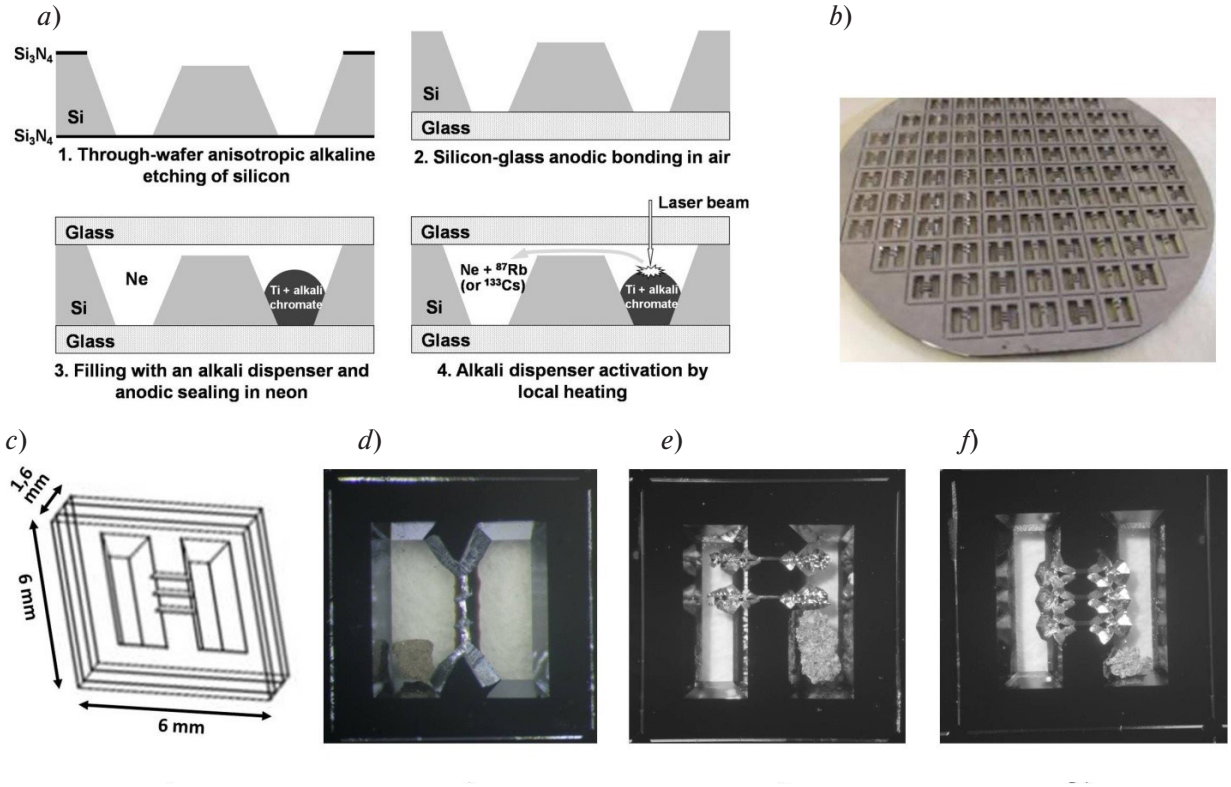

Fig. 6. Results of MEMS vapor cells fabrication: cells fabrication process (*a*), bonded glass-silicon-glass wafer (*b*), basic cell design (*c*), first microfabricated atomic cell prototype (*d*), ^{133}Cs-Ne vapor cell (*e*) and ^{87}Rb-Ne vapor cell (*f*)

to the process. First, 200 nm thick silicon nitride layers were deposited on both sides of the wafer, and a mask pattern was formed on one side by direct photolithography and Si_3N_4 plasma etching. An array of the through-wafer cavities and the filtration channels (V-grooves trenches with a depth of 280 μm) was formed in the silicon wafer by anisotropic wet etching in potassium hydroxide solutions. To enhance the cells performance, several filtration channels designs and alkaline etching techniques have been developed. At the next stage, the nitride layer was removed, followed by anodic bonding of the silicon wafer to the bottom glass. Bonding was carried out in air at 400 °C and 800 V for 30 minutes. Then, Cs- or Rb-containing microsources were inserted in the dispenser cavities of every cell. As sources of alkali metal vapors, solid micropills made by sintering titanium powders with 7 % rubidium or caesium bichromate was used.

The vacuum-tight bonding of the top glass wafer was carried out at 250 °C according to the scheme shown in Fig. 3*a*. Previously, a thin-film aluminum cathode was sputtered on the reverse side of the top glass wafer. Neon at a pressure of 100–400 Torr was used as a buffer gas. The specific value of the neon pressure in the cells for CSAC was selected on the basis of previous experimental work [23]. Anodic sealing at such neon pressures differs from sealing in a standard air atmosphere due to the occurrence of a gas breakdown in our bonding chamber at voltage of about 400 V. For this reason bonding voltage was reduced to 350 V, but bonding duration was increased. The sequence of operations for cells encapsulation with LK5 lid was as follows: annealing and degassing the wafers with a gap between them in vacuum (350 °C, 0.5 mTorr, 1 hour), cooling to room temperature, introduction of neon, annealing to 250 °C, applying the contact force on wafers, anodic bonding for 2 hours, cooling. After sealing, the aluminum cathode coating was removed by wet etching (both glass wafers remained transparent).

At the final stage of the cells fabrication process, the bonded glass-silicon-glass wafer was divided into separate chips, followed by the activation of the alkali dispensers by local laser heating according to a well-known technique [14].

Fig. 6*d* shows the photo of the first cell filled with ^{87}Rb vapor and Ne gas under the pressure of 200 Torr fabricated by authors in 2014. The cell cavities thickness was 400 μm. The relative short-term frequency stability was estimated as $1.4 \cdot 10^{-10}$ $s^{-1/2}$ [15].

Fig. 6*e* and Fig. 6*f* show the photos of the ^{133}Cs and ^{87}Rb vapor cells with the Ne pressure of 300 Torr, respectively. These cells have improved design and 600 μm thick cavities. Preliminary experiments have shown that cell parameters dispersion for the width and intensity of the Hanle and CPT signals is from 30 to 50 %, which can be explained by differences in the modes of laser activation of cells. Relative short-term frequency stability for best samples is $2.5 \cdot 10^{-11}$ $s^{-1/2}$ [13].

Conclusion

We analyzed the dependence of the chip-scale atomic clock short-term and long-term frequency stability on the structural and technological parameters of the MEMS alkali vapor cells with buffer gases or anti-relaxation wall coatings. As the analysis showed, to improve these parameters, it is desirable to reduce the temperature of the anode bonding of silicon and glass used for MEMS cells sealing, since the exact composition of the cell inner atmosphere significantly depends on the results of this operation. Two alternative materials, LK5 glass and SO-33M glass-ceramic, with increased ionic conductivity compared to the conventional glasses used in MEMS technology have been experimentally investigated to develop low-temperature anodic bonding with silicon, fused quartz, and to each other.

Transparent lithium aluminosilicate glass-ceramics SO-33M with a near-zero coefficient of thermal expansion provided acceptable quality of anodic sealing at a temperature of 150 °C. Intermediate thin-film polysilicon layers were used to bond the glass-ceramic wafers to each other and to fused quartz. The prototypes of MEMS cells with optical windows made of glass-ceramic and fused quartz were made. The developed technology can be promising for the fabrication of alkali vapor cells with organic anti-relaxation coating.

We developed a technology of MEMS atomic cells containing rubidium or caesium vapors in an atmosphere of neon buffer gas. Two-chamber silicon cells containing an optical cavity, shallow filtration channels and a technical container for a solid alkali microdispenser have been fabricated. We sealed the cells by means of silicon-to-LK5-glass anodic bonding at a temperature of 250 °C. The best microfabricated cells allowed us to obtain estimates of the CPT-resonance frequency stability at the level of $2.5 \cdot 10^{-11}$ at 1 s. An acceptable reproducibility of the parameters of the cell from various series confirms the feasibility of introducing the developed MEMS technology in the implementation of small-sized quantum frequency standard.

This work was carried out in Peter the Great St.Petersburg Polytechnic University and was supported by a grant of Russian Science Foundation (project No. 20-19-00146).

REFERENCES

1. **Kitching J.** Chip-scale atomic devices. *Applied Physics Reviews*, 2018, No. 5, 031302. DOI: 10.1063/1.5026238

2. **Lozov R.K., Baranov A.A., Ermak S.V., Semenov V.V.** Comparison of orientational error of an optically pumped quantum sensor in on-board equipment of Galileo and GPS satellite systems. *Journal of Physics: Conference Series*, 2019, Vol. 1236, 012077. DOI: 10.1088/1742-6596/1236/1/012077

3. **Borisevich E., Korolev A., Lozov R.** The orbits shape influence of the navigation satellite systems on positioning accuracy. *International Youth Conference on Electronics, Telecommunications and Information Technolo-*

gies. Springer Proceedings in Physics, Springer, Cham., 2021, Vol. 255, Pp. 761–775. DOI: 10.1007/978-3-030-58868-7_83

4. **Bobrov M.A., Blokhin S.A., Maleev N.A., Blokhin A.A., Vasyl'ev A.P., Kuzmenkov A.G., Pazgalev A.S., Petrenko M.V., Dmitriev S.P., Vershovskii A.K., Ustinov V.M., Novikov I.I., Karachinskii L.Ya.** Optically pumped non-zero field magnetometric sensor for the magnetoencephalographic systems using intra-cavity contacted VCSELs with rhomboidal oxide current aperture. *Journal of Physics: Conference Series*, 2020, Vol. 1697, 012175. DOI: 10.1088/1742-6596/1697/1/012175

5. **Knapkiewicz P.** Alkali vapor MEMS cells technology toward high-vacuum self-pumping MEMS cell for atomic spectroscopy. *Micromachines*, 2018, No. 9, 405. DOI: 10.3390/mi9080405

6. **Rushton J.A., Aldous M., Himsworth M.D.** Contributed review: The feasibility of a fully miniaturized magneto-optical trap for portable ultracold quantum technology. *Review of Scientific Instruments*, 2014, Vol. 85, 121501. DOI: 10.1063/1.4904066

7. **Knappe S., Schwindt P.D.D., Gerginov V., Shah V., Hollberg L., Kitching J., Liew L., Moreland J.** Microfabricated atomic clocks at NIST. *Proceedings of the 36th Annual Precise Time and Time Interval Systems and Applications Meeting*, Washington, D.C., Dec. 2004, Pp. 383–392.

8. **Petremand Y., Affolderbach C., Straessle R., Pellaton M., Briand D., Mileti G., de Rooij N.F.** Microfabricated rubidium vapour cell with a thick glass core for small-scale atomic clock applications. *Journal of Micromechanics and Microengineering*, 2012, Vol. 22, No. 2, 025013. DOI: 10.1088/0960-1317/22/2/025013

9. **Gorecki C.** Development of first European chip-scale atomic clocks: technologies, assembling and metrology. *Procedia Engineering*, 2012, No. 47, Pp. 898–903. DOI: 10.1016/j.proeng.2012.09.292

10. **Vicarini R., Maurice V., Abdel Hafiz M., Rutkowski J., Gorecki C., Passilly N., Ribetto L., Gaff V., Volant V., Galliou S., Boudot R.** Demonstration of the mass-producible feature of a Cs vapor microcell technology for miniature atomic clocks. *Sensors and Actuators A*, 2018, Vol. 280, Pp. 99–106. DOI: 10.1016/j.sna.2018.07.032

11. **Vanier J., Levine M., Kendig S., Janssen D., Everson C., Delaney M.** Practical realization of a passive coherent population trapping frequency standard. *IEEE Transactions on Instrumentation and Measurement*, 2005, Vol. 54, No. 6, Pp. 2531–2539. DOI: 10.1109/TIM.2005.858120

12. **Knappe S.** MEMS Atomic clocks. *Comprehensive Microsystems*, 2008, Vol. 3, Pp. 571–612.

13. **Bobrov M.A., Blokhin S.A., Maleev N.A., Blokhin A.A., Vasyl'ev A.P., Kuzmenkov A.G., Gladyshev A.G., Novikov I.I., Petrenko M.V., Ospennikov A.M., Ermak S.V., Ustinov V.M.** Effect of coherent population trapping in a compact microfabricated Cs gas cell pumped by intra-cavity contacted VCSELs with rhomboidal oxide current aperture. *Journal of Physics: Conference Series*, 2019, Vol. 1400, 077014. DOI: 10.1088/1742-6596/1400/7/077014

14. **Hasegawa M., Chutani R.K., Gorecki C., Boudot R., Dziuban P., Giordano V., Clatot S., Mauri L.** Microfabrication of cesium vapor cells with buffer gas for MEMS atomic clocks. *Sensors and Actuators A*, 2011, Vol. 167, Pp. 594–601. DOI: 10.1016/j.sna.2011.02.039

15. **Ermak S.V., Semenov V.V., Piatyshev E.N., Kazakin A.N., Komarevtsev I.M., Velichko E.N., Davydov V.V., Petrenko M.V.** Microfabricated cells for chip-scale atomic clock based on coherent population trapping: Fabrication and investigation. *St. Petersburg Polytechnical University Journal: Physics and Mathematics*, 2015, No. 1, Pp. 37–41. DOI: 10.1016/j.spjpm.2015.03.003

16. **Knappe S., Schwind P.D.D., Shah V., Hollberg L., Kitching J., Liew L., Moreland J.** A chip-scale atomic clock based on 87Rb with improwed frequency stability. *Optics Express*, 2005, Vol. 13, No. 4, Pp. 1249–1253.

17. **Straessle R., Pellaton M., Affolderbach C., Pétremand Y., Briand D., Mileti G., de Rooij N.F.** Microfabricated alkali vapor cell with anti-relaxation wall coating. *Applied Physics Letters*, 2014, Vol. 105, 043502. DOI: 10.1063/1.4891248

18. **Knapkiewicz P.** Technological assessment of MEMS alkali vapor cells for atomic references. *Micromachines*, 2019, No. 10, 25. DOI: 10.3390/mi10010025

19. **Dziuban J.A.** Bonding in microsystem technology. *Springer Series in Advanced Microelectronics*, 2006, Vol. 24, 331 p.

20. **Wallis G., Pomerantz D.** Field assisted glass-metal sealing. *Journal of Applied Physics*, 1969, Vol. 40, No. 10, Pp. 3946–3949.

21. **Berthold A., Nicola L., Sarro P.M., Vellekoop M.J.** Glass-to-glass anodic bonding with standard IC technology thin films as intermediate layers. *Sensors and Actuators*, 2000, Vol. 82, Pp. 224–228.

22. **van Elp J., Giesen P.T.M., van der Velde J.J.** Anodic bonding using the low expansion glass ceramic Zerodur. *Journal of Vacuum Science & Technology B*, 2005, Vol. 23, No. 1, Pp. 96–98. DOI: 10.1116/1.1839912

23. **Fedorov M.I., Ermak S.V., Petrenko M.V., Pyatyshev E.N., Semenov V.V.** Investigation of coherent population trapping signals in 87Rb cells with buffer gas. *Journal of Physics: Conference Series*, 2016, Vol. 769, 012046. DOI: 10.1088/1742-6596/769/1/012046

24. **Gerginov V., Knappe S., Shah V., Schwind P.D.D., Hollberg L., Kitching J.** Long-term frequency instability of atomic frequency references based on coherent population trapping and microfabricated vapor cells. *Journal of Optical Society of America B*, 2006, Vol. 23, No. 4, Pp. 593–597.

25. **Kobtsev S., Radnatarov D., Khripunov S., Popkov I., Andryushkov V., Steshchenko T.** Stability properties of an Rb CPT atomic clock with buffer-gas-free cells under dynamic excitation. *Journal of the Optical Society of America B*, 2019, Vol. 36, No. 10, Pp. 2700–2704, DOI: 10.1364/JOSAB.36.002700

26. **Chi H., Quan W., Zhang J., Zhao L., Fang J.** Advances in anti-relaxation coatings of alkali-metal vapor cells. *Applied Surface Science*, 2020, Vol. 501, 143897. DOI: 10.1016/j.apsusc.2019.143897

27. **Ji Y., Shang J., Gan Q., Wu L.** Wafer-level micro alkali vapor cells with anti-relaxation coating compatible with MEMS packaging for chip-scale atomic magnetometers. *2017 IEEE 67th Electronic Components and Technology Conference* (*ECTC*), 2017, Pp. 2116–2120. DOI: 10.1109/ECTC.2017.136

28. **Norton F.J.** Permeation of Gases through Solids. *Journal of Applied Physics*, 1957, No. 28, Pp. 34–39. DOI: 10.1063/1.1722570

29. **Abdullah S., Affolderbach C., Gruet F., Mileti G.** Aging studies on micro-fabricated alkali buffer-gas cells for miniature atomic clocks. *Applied Physics Letters*, 2015, Vol. 106, 163505.

30. **Dellis A.T., Shah V., Donley E.A., Knappe S., Kitching J.** Low helium permeation cells for atomic microsystems technology. *Optics Letters*, 2016, Vol. 41, No. 12, Pp. 2775–2778. DOI: 10.1364/OL.41.002775

31. **Sinev L.S., Ryabov V.T.** Reducing thermal mismatch stress in anodically bonded silicon-glass wafers: theoretical estimation. *Journal of Micro/Nanolithography, MEMS, and MOEMS*, 2017, Vol. 16, No. 1, 015003. DOI: 10.1117/1.JMM.16.1.015003

32. **Dymshits O., Shepilov M., Zhilin A.** Transparent glass-ceramics for optical applications, 2017, *MRS Bulletin*, Vol. 42, Pp. 200–205. DOI: 10.1557/mrs.2017.29

33. **Hu X., Mackowiak P., Baeuscher M., Zhang Y., Wang B., Hansen U.** Low stress solution of anodic bonding technology with SW-YY glass for sensitive MEMS. *2018 IEEE 20th Electronics Packaging Technology Conference*, 2018, Pp. 251–255. DOI: 10.1109/EPTC.2018.8654362

34. **Shoji S., Kikuchi H., Torigoe H.** Anodic bonding below 180 °C for packaging and assembling of MEMS using lithium aluminosilicate-β-quartz glass-ceramic. *Proceedings IEEE the 10th Annual International Workshop on Micro Electro Mechanical Systems. An Investigation of Micro Structures, Sensors, Actuators, Machines and Robots*, 1997, Pp. 482–487. DOI: 10.1109/MEMSYS.1997.581907

Received 08.06.2021.

СПИСОК ЛИТЕРАТУРЫ

1. **Kitching J.** Chip-scale atomic devices // Applied Physics Reviews. 2018. No. 5. 031302. DOI: 10.10-63/1.5026238

2. **Lozov R.K., Baranov A.A., Ermak S.V., Semenov V.V.** Comparison of orientational error of an optically pumped quantum sensor in on-board equipment of Galileo and GPS satellite systems // J. of Physics: Conf. Ser. 2019. Vol. 1236. 012077. DOI: 10.1088/1742-6596/1236/1/012077

3. **Borisevich E., Korolev A., Lozov R.** The orbits shape influence of the navigation satellite systems on positioning accuracy // Internat. Youth Conf. on Electronics, Telecommunications and Information Technologies. Springer Proceedings in Physics. Springer, Cham., 2021. Vol. 255. Pp. 761–775. DOI: 10.1007/978-3-030-58868-7_83

4. **Bobrov M.A., Blokhin S.A., Maleev N.A., Blokhin A.A., Vasyl'ev A.P., Kuzmenkov A.G., Pazgalev A.S., Petrenko M.V., Dmitriev S.P., Vershovskii A. K., Ustinov V.M., Novikov I.I., Karachinskii L.Ya.** Optically pumped non-zero field magnetometric sensor for the magnetoencephalographic systems using intra-cavity contacted VCSELs with rhomboidal oxide current aperture // J. of Physics: Conf. Ser. 2020. Vol. 1697. 012175. DOI: 10.1088/1742-6596/1697/1/012175

5. **Knapkiewicz P.** Alkali vapor MEMS cells technology toward high-vacuum self-pumping MEMS cell for atomic spectroscopy // Micromachines. 2018. No. 9. 405. DOI: 10.3390/mi9080405

6. **Rushton J.A., Aldous M., Himsworth M.D.** Contributed review: The feasibility of a fully miniaturized magneto-optical trap for portable ultracold quantum technology // Review of Scientific Instruments. 2014. Vol. 85. 121501. DOI: 10.1063/1.4904066

7. **Knappe S., Schwindt P.D.D., Gerginov V., Shah V., Hollberg L., Kitching J., Liew L., Moreland J.** Microfabricated atomic clocks at NIST // Proc. of the 36th Annual Precise Time and Time Interval Systems and Applications Meeting. Washington, D.C., Dec. 2004. Pp. 383–392.

8. **Petremand Y., Affolderbach C., Straessle R., Pellaton M., Briand D., Mileti G., de Rooij N.F.** Microfabricated rubidium vapour cell with a thick glass core for small-scale atomic clock applications // J. of Micromechanics and Microengineering. 2012. Vol. 22. No. 2. 025013. DOI: 10.1088/0960-1317/22/2/025013

9. **Gorecki C.** Development of first European chip-scale atomic clocks: technologies, assembling and metrology // Procedia Engineering. 2012. No. 47. Pp. 898–903. DOI: 10.1016/j.proeng.2012.09.292

10. **Vicarini R., Maurice V., Abdel Hafiz M., Rutkowski J., Gorecki C., Passilly N., Ribetto L., Gaff V., Volant V., Galliou S., Boudot R.** Demonstration of the mass-producible feature of a Cs vapor microcell technology for miniature atomic clocks // Sensors and Actuators A. 2018. Vol. 280. Pp. 99–106. DOI: 10.1016/j.sna.2018.07.032

11. **Vanier J., Levine M., Kendig S., Janssen D., Everson C., Delaney M.** Practical realization of a passive coherent population trapping frequency standard // IEEE Transactions on Instrumentation and Measurement. 2005. Vol. 54. No. 6. Pp. 2531–2539. DOI: 10.1109/TIM.2005.858120

12. **Knappe S.** MEMS atomic clocks // Comprehensive Microsystems. 2008. Vol. 3. Pp. 571–612.

13. **Bobrov M.A., Blokhin S.A., Maleev N.A., Blokhin A.A., Vasyl'ev A.P., Kuzmenkov A.G., Gladyshev A.G., Novikov I.I., Petrenko M.V., Ospennikov A.M., Ermak S.V., Ustinov V.M.** Effect of coherent population trapping in a compact microfabricated Cs gas cell pumped by intra-cavity contacted VCSELs with rhomboidal oxide current aperture // J. of Physics: Conf. Ser. 2019. Vol. 1400. 077014. DOI: 10.1088/1742-6596/1400/7/077014

14. **Hasegawa M., Chutani R.K., Gorecki C., Boudot R., Dziuban P., Giordano V., Clatot S., Mauri L.** Microfabrication of cesium vapor cells with buffer gas for MEMS atomic clocks // Sensors and Actuators A. 2011. Vol. 167. Pp. 594–601. DOI: 10.1016/j.sna.2011.02.039

15. **Ermak S.V., Semenov V.V., Piatyshev E.N., Kazakin A.N., Komarevtsev I.M., Velichko E.N., Davydov V.V., Petrenko M.V.** Microfabricated cells for chip-scale atomic clock based on coherent population trapping: Fabrication and investigation // St. Petersburg Polytechnical University Journal. Physics and Mathematics. 2015. No. 1. Pp. 37–41. DOI: 10.1016/j.spjpm.2015.03.003

16. **Knappe S., Schwind P.D.D., Shah V., Hollberg L., Kitching J., Liew L., Moreland J.** A chip-scale atomic clock based on 87Rb with improwed frequency stability // Optics Express. 2005. Vol. 13. No. 4. Pp. 1249–1253.

17. **Straessle R., Pellaton M., Affolderbach C., Pétremand Y., Briand D., Mileti G., de Rooij N.F.** Microfabricated alkali vapor cell with anti-relaxation wall coating // Applied Physics Letters. 2014. Vol. 105. 043502. DOI: 10.1063/1.4891248

18. **Knapkiewicz P.** Technological assessment of MEMS alkali vapor cells for atomic references // Micromachines. 2019. No. 10. 25. DOI: 10.3390/mi10010025

19. **Dziuban J.A.** Bonding in microsystem technology // Springer Series in Advanced Microelectronics. 2006. Vol. 24. 331 p.

20. **Wallis G., Pomerantz D.** Field assisted glass-metal sealing // J. of Applied Physics. 1969. Vol. 40. No. 10. Pp. 3946–3949.

21. **Berthold A., Nicola L., Sarro P.M., Vellekoop M.J.** Glass-to-glass anodic bonding with standard IC technology thin films as intermediate layers // Sensors and Actuators. 2000. Vol. 82. Pp. 224–228.

22. **van Elp J., Giesen P.T.M., van der Velde J.J.** Anodic bonding using the low expansion glass ceramic Zerodur // J. of Vacuum Science & Technology B. 2005. Vol. 23. No. 1. Pp. 96–98. DOI: 10.1116/1.1839912

23. **Fedorov M.I., Ermak S.V., Petrenko M.V., Pyatyshev E.N., Semenov V.V.** Investigation of coherent population trapping signals in 87Rb cells with buffer gas // J. of Physics: Conf. Ser. 2016. Vol. 769. 012046. DOI: 10.1088/1742-6596/769/1/012046

24. **Gerginov V., Knappe S., Shah V., Schwind P.D.D., Hollberg L., Kitching J.** Long-term frequency instability of atomic frequency references based on coherent population trapping and microfabricated vapor cells // J. of Optical Society of America B. 2006. Vol. 23. No. 4. Pp. 593–597.

25. **Kobtsev S., Radnatarov D., Khripunov S., Popkov I., Andryushkov V., Steshchenko T.** Stability properties of an Rb CPT atomic clock with buffer-gas-free cells under dynamic excitation // J. of the Optical Society of America B. 2019. Vol. 36. No. 10. Pp. 2700–2704. DOI: 10.1364/JOSAB.36.002700

26. **Chi H., Quan W., Zhang J., Zhao L., Fang J.** Advances in anti-relaxation coatings of alkali-metal vapor cells // Applied Surface Science. 2020. Vol. 501. 143897. DOI: 10.1016/j.apsusc.2019.143897

27. **Ji Y., Shang J., Gan Q., Wu L.** Wafer-level micro alkali vapor cells with anti-relaxation coating compatible with MEMS packaging for chip-scale atomic magnetometers // 2017 IEEE 67th Electronic Components and Technology Conf. 2017. Pp. 2116–2120. DOI: 10.1109/ECTC.2017.136

28. **Norton F.J.** Permeation of gases through solids // J. of Applied Physics. 1957. No. 28. Pp. 34–39. DOI: 10.1063/1.1722570

29. **Abdullah S., Affolderbach C., Gruet F., Mileti G.** Aging studies on micro-fabricated alkali buffer-gas cells for miniature atomic clocks // Applied Physics Letters. 2015. Vol. 106. 163505.

30. **Dellis A.T., Shah V., Donley E.A., Knappe S., Kitching J.** Low helium permeation cells for atomic microsystems technology // Optics Letters. 2016. Vol. 41. No. 12. Pp. 2775–2778. DOI: 10.1364/OL.41.002775

31. **Sinev L.S., Ryabov V.T.** Reducing thermal mismatch stress in anodically bonded silicon-glass wafers: theoretical estimation // J. of Micro/Nanolithography, MEMS, and MOEMS. 2017. Vol. 16. No. 1. 015003. DOI: 10.1117/1.JMM.16.1.015003

32. **Dymshits O., Shepilov M., Zhilin A.** Transparent glass-ceramics for optical applications // MRS Bulletin. 2017. Vol. 42. Pp. 200–205. DOI: 10.1557/mrs.2017.29

33. **Hu X., Mackowiak P., Baeuscher M., Zhang Y., Wang B., Hansen U.** Low stress solution of anodic bonding technology with SW-YY glass for sensitive MEMS // Proc. of the 20th Electronics Packaging Technology Conf. 2018. Pp. 251–255. DOI: 10.1109/EPTC.2018.8654362

34. **Shoji S., Kikuchi H., Torigoe H.** Anodic bonding below 180 °C for packaging and assembling of MEMS using lithium aluminosilicate-β-quartz glass-ceramic // Proc. IEEE the 10th Annual International Workshop on Micro Electro Mechanical Systems. An Investigation of Micro Structures, Sensors, Actuators, Machines and Robots. 1997. Pp. 482–487. DOI: 10.1109/MEMSYS.1997.581907

Статья поступила в редакцию 08.06.2021.

THE AUTHORS / СВЕДЕНИЯ ОБ АВТОРАХ

Kazakin Alexei N.
Казакин Алексей Николаевич
E-mail: kazakin75@gmail.com

Kleimanov Roman V.
Клейманов Роман Валерьевич
E-mail: kleimanovrv@mail.ru

Korshunov Andrei V.
Коршунов Андрей Васильевич
E-mail: korshunov@spbstu.ru

Akulshin Yuri D.
Акульшин Юрий Дмитриевич
E-mail: akulshin_yud@spbstu.ru

Shashkin Aleksandr V.
Шашкин Александр Викторович
E-mail: shashkin@goi.ru